BIGLOBAL STABILITY ANALYSIS OF STENOTIC FLOW

Robin Pitt, Spencer Sherwin
Department of Aeronautics,
Imperial College
London, SW7 2AZ, United Kingdom
robin.pitt@imperial.ac.uk, s.sherwin@imperial.ac.uk

Vassilis Theofilis
Universidad Politécnica de Madrid,
Escuela Tecnica Superior Ingenieros Aeronáuticos,
Departamento de Motopropulsión y Termofluidodinámica
Pza. Cardenal Cisneros, 3
E-28040 Madrid, Spain
vassilis@torroja.dmt.upm.es

ABSTRACT

A BiGlobal stability analysis technique based on spectral/*hp* element technology is discussed, and applied to the biomedically important problem of the flow through a constricted channel. Results for both steady flows and the Floquet analysis of time periodic flow are presented. In the steady case the onset of three-dimensionality is investigated, and the effect of stenosis extent is examined. In the periodic case preliminary results concerning the initial bifurcation to asymmetry are presented.

INTRODUCTION

Atherosclerosis, the formation of plaques within the arterial wall, continues to be a major cause of death in the developed world. The associated narrowing, or stenosis, of the artery causes a significant reduction in the blood flow supplied to downstream vessels. A further life threatening condition may occur if the plaque ruptures. This can cause thrombosis of the affected vessel or particles to become lodged in smaller vessels, possibly inducing myocardial infarction or stroke.

While the fluid mechanical factors contributing to the initiation of sclerotic regions (the process of atherogenesis) are fairly well understood (Caro et al., 1971, Nerem and Cornhill, 1980), those playing a part in plaque rupture are less so. Study of the flow within relatively highly occluded artery models is therefore motivated, in order to characterise the flow conditions that arise in the immediate neighbourhood of the plaque.

Physiological flow conditions within most large healthy arteries are normally pulsatile in nature but typically operate in a laminar unsteady flow regime. However, the solution of flow in stenotic geometries, such as that shown in Figure 1, provides an interesting additional fluid mechanical challenge since, for a given flow rate, the local Reynolds number of the flow increases as the inverse of the vessel diameter reduction. Therefore even at moderate levels of occlusion transitional Reynolds numbers are possible.

Numerically, the high local velocities at the stenosis and the need for a fine discretisation results in a greatly reduced time-step when considering the CFL stability restriction associated with an explicit treatment of the advection operator. The resulting high computational time can make a thorough investigation of the many parameters involved such as geometry, inflow waveform and Reynolds number, prohibitively expensive.

A BiGlobal stability analysis (Theofilis, 2003) can alternatively be employed to study the laminar instabilities and transitions occurring within the stenosis. Unlike classical stability analysis where a one-dimensional base flow is considered and the other two spatial directions are harmonically expanded, in the BiGlobal stability analysis both the basic state and the amplitude functions of small-amplitude disturbances superimposed upon the basic state are non-periodic *two-dimensional* functions; the third spatial direction is considered homogeneous and expanded harmonically in Fourier wavenumbers β. The method is thus suited to investigation of the stability of flows with homogeneity of geometry in one dimension, for example channel, cylinder or axisymmetric geometries. In this paper, the geometry we consider is a plane channel geometry, infinite in the z-direction, with a prescribed contraction and subsequent re-expansion in the y-direction.

In this paper we first present a brief introduction to the numerical method involved in this BiGlobal stability analysis, before demonstrating how the stability of stenotic flows is affected by the Reynolds number, by the contraction ratio of the stenosis and by the addition of pulsatility to the inflow. These results are given in terms of the value of the dominant eigenvalue, the shape of the dominant eigenmode, and the spanwise wavenumber β.

NUMERICAL METHODOLOGY

We take as the governing equations for arterial flow the incompressible Newtonian Navier-Stokes equations

$$\frac{\partial \mathbf{u}}{\partial t} = -\mathbf{N}(\mathbf{u}) - \frac{1}{\rho}\nabla p + \frac{1}{Re}\nabla^2 \mathbf{u} \ \ in\ \Omega \qquad (1)$$

together with the continuity requirement

$$\nabla \cdot \mathbf{u} = 0 \ \ in\ \Omega \qquad (2)$$

where $\mathbf{u}$ is the three dimensional velocity field, ρ and p are the fluid density and pressure respectively, and Re is the Reynolds number $Re = UD/\nu$. For our purposes the length

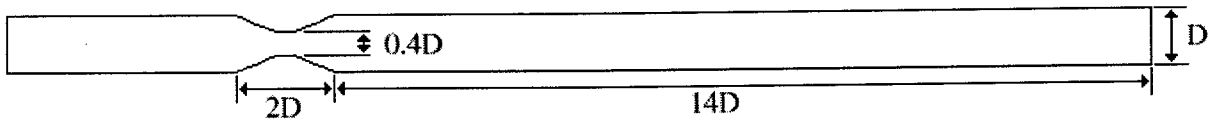

Figure 1: Geometry of 60% occluded channel stenosis model

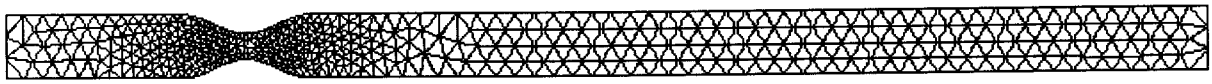

Figure 2: Mesh used for base flow and stability calculations on 60% stenosis

scale D taken in the definition of the Reynolds number is the channel height (see Figure 1), and the velocity scale U the temporally and spatially averaged inflow velocity ($\bar{U}$). $\mathbf{N}(\mathbf{u})$ is the nonlinear advection operator $\mathbf{N}(\mathbf{u}) = (\mathbf{u} \cdot \nabla)\mathbf{u}$. Equation (1) is subject to no-slip boundary conditions at the walls, a prescribed velocity at the inflow (steady or periodic), and conditions of zero pressure and zero outward normal derivatives of velocity at the outflow.

We decompose the instantaneous flow field into a two-dimensional base flow, $\mathbf{U}$, and a small perturbation $\mathbf{u}'$:

$$\mathbf{u}(x, y, z, t) = \mathbf{U}(x, y, t) + \mathbf{u}'(x, y, z, t) \tag{3}$$

$\mathbf{U}$ is a solution of equation (1) on a two dimensional computational domain, Ω, which is invariant in the z-direction (the direction of homogeneity). This base flow may be steady ($\partial\mathbf{U}/\partial t = 0$), or may be periodic in time ($\mathbf{U}(x, y, t) = \mathbf{U}(x, y, t + T)$ for all t and finite period T). The periodic case requires the use of Floquet stability analysis.

Placing the definition (3) into (1) and neglecting as small the terms corresponding to the product of the small perturbations we arrive at the linearised Navier-Stokes equations:

$$\frac{\partial \mathbf{u}'}{\partial t} = -\mathbf{DN}(\mathbf{u}') - \frac{1}{\rho}\nabla p' + \frac{1}{Re}\nabla^2 \mathbf{u}' \ \ in\ \Omega \tag{4}$$

where $\mathbf{u}'$ is again constrained to be divergence free (satisfying (2)), a situation which is maintained by the perturbation pressure field p'. $\mathbf{u}'$ is constrained to be zero at the Dirichlet boundaries and to observe the same outflow condition as imposed previously on $\mathbf{u}$, to ensure that the disturbance flow satisfies the same boundary conditions as the complete flow. $\mathbf{DN}$ is the linearised advection operator:

$$\mathbf{DN} = (\mathbf{u}' \cdot \nabla)\mathbf{U} + (\mathbf{U} \cdot \nabla)\mathbf{u}' \tag{5}$$

For the case of steady base flow $\mathbf{DN}$ is constant, and in the periodic case it is time periodic also, with the same period T as the base flow. Equation (4) can be written more compactly as:

$$\frac{\partial \mathbf{u}'}{\partial t} = \mathbf{L}(\mathbf{u}') \tag{6}$$

where the linear operator $\mathbf{L}(\mathbf{u}')$ represents the right hand side of (4), and is again periodic with periodic base flow.

Solutions of (4) comprise a sum of exponential functions of the form $\tilde{\mathbf{u}}(x, y, z, t)e^{\sigma t}$. The modes $\tilde{\mathbf{u}}$ are time periodic when the base flow is periodic; in this case they are referred to as the 'Floquet modes' of operator $\mathbf{L}$. For steady base flows we consider the exponents σ. A mode is linearly unstable (will grow in time) if the real part of this exponent is greater than zero. Conversely, in the study of periodic flows we generally consider the 'Floquet multipliers', $\mu = e^{\sigma T}$, which give a measure of the growth of the perturbation mode throughout one base flow cycle. The corresponding mode becomes unstable if the magnitude $|\mu|$ becomes greater than unity.

A simplification to the form of $\mathbf{u}'$ can be made due to the homogeneity of the domain and the assumption that it is infinite in the z-direction, by expressing the general perturbation as the Fourier integral (Barkley and Henderson, 1996):

$$\mathbf{u}'(x, y, z, t) = \int_{-\infty}^{\infty} \hat{\mathbf{u}}(x, y, \beta, t)e^{i\beta z} d\beta \tag{7}$$

This also has the effect of modifying the gradient operator wherever it is used so that $\nabla \equiv (\partial/\partial x, \partial/\partial y, -i\beta)$. The linearity of (4) ensures that perturbation modes with different spanwise wavenumber β do not couple, and thus can be calculated separately.

We use essentially the same method to find the dominant (most unstable) exponents and Floquet multipliers in both the steady and periodic cases. We define an operator $\mathbf{A}$ describing the evolution of $\mathbf{u}'$ over the period T (Schatz et al., 1995):

$$\mathbf{u}'_{n+1} = \mathbf{A}(\mathbf{u}'_n) \tag{8}$$

where $\mathbf{u}'_n$ is the perturbation field after n base flow cycles. In the case of periodic base flow then $\mathbf{A}$ is equivalent to the linearised Poincaré map corresponding to the orbit of the base flow. The action of $\mathbf{A}$ is the time integrated effect of the operator $\mathbf{L}$ on an initially infinitesimal perturbation over one period:

$$\mathbf{A}(\mathbf{u}') = \exp\left(\int_0^T \mathbf{L}(\mathbf{u}')dt\right) \tag{9}$$

The Floquet multipliers are the eigenvalues of $\mathbf{A}$, and the eigenmodes of $\mathbf{A}$ correspond to the Floquet modes $\tilde{\mathbf{u}}$. The Floquet modes depend on the point taken to be the start of the period; the Floquet multipliers do not. In the case of steady base flow then an arbitrary time period T is chosen for computational convenience and the relevant exponents reclaimed via the relation $\sigma = (\ln(\mu)/T)$. The eigenmodes calculated are then time invariant, and give the initial form of any instability arising.

The action of $\mathbf{A}$ is approximated by integrating (4) over $T/\Delta t$ time-steps. This is performed by modification of an existing spectral/hp element solver for solution of the Navier-Stokes equations (1) on three-dimensional domains with z-direction homogeneity (Tuckerman and Barkley, 2000). The non-linear advection operator $\mathbf{N}$ must be replaced with its

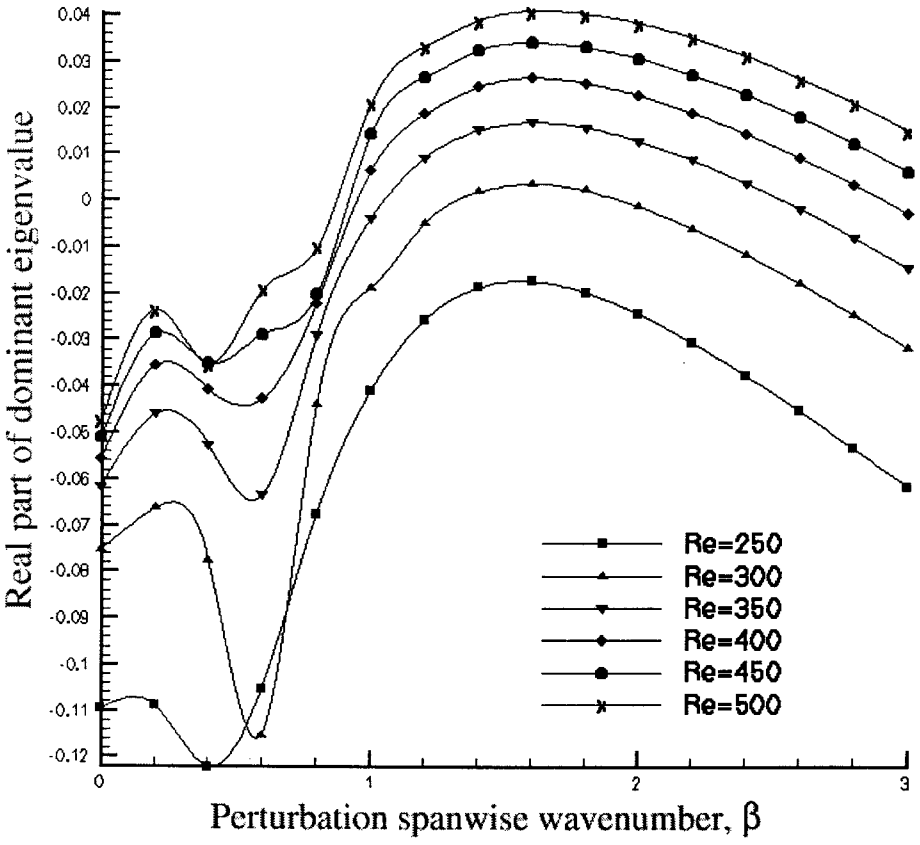

Figure 3: Plot of real part of dominant eigenvalue against spanwise wavenumber β for 60% stenosis at a range of Reynolds numbers

Figure 4: Out of plane perturbation velocity of dominant eigenmode at $\beta = 1.6$, $Re = 300$

linearised counterpart **DN**, and the gradient operator must be modified as previously stated.

For Floquet stability analysis the periodic base flow is required at each of the time steps. Its periodicity suggests the use of a Fourier series in time to represent it, facilitated by using an FFT algorithm over a number of slices of the base flow at the start of the calculation and subsequently interpolating at each step. For the work in this paper 32 base flow slices were used. All of the base flows were calculated using an unsteady two-dimensional spectral/*hp* Navier-Stokes solver, on the same meshes as used for the subsequent stability analysis.

The eigenvalues of **A** are found via the time integration of (4), using the Arnoldi method, avoiding the high memory requirements of a direct method. For the work in this paper a low Krylov subspace dimension was used, but sufficiently large for converged eigenvalues to be obtained. The spectral/*hp* method of spatial discretisation, chosen for this work for its favourable convergence properties, is described in the context of stability analysis by Theofilis et al. (2002). The calculations in this paper have been performed on stenoses of 60%, 78% and 90% occlusion, using meshes of 840, 1054 and 1187 elements respectively. All calculations were performed using 7 modes, corresponding to a maximum expansion base polynomial order of 6. The mesh used for the 60% stenosis case is depicted in Figure 2. Each curve of the stenosis is described by 17 points, through which a cubic spline is interpolated for the purposes of the calculation. Analytically, the top and bottom curves are each divided into two halves, and described by a fifth order polynomial with zero derivative at the end and centre of the stenosis.

RESULTS AND DISCUSSION

Instability analysis of steady basic flow

Sobey and Drazin (1986) discuss the two-dimensional flow through a stenotic channel in the language of bifurcation theory. At sufficiently low Reynolds number the steady flow through a stenotic channel has a unique, symmetric solution. As *Re* is increased a critical value is reached and the flow becomes asymmetric, sometimes referred to as the Coanda effect. Sobey and Drazin performed a number of numerical and experimental investigations to isolate this pitchfork bifurcation.

We have turned our BiGlobal stability analysis technique to the exploration of the linear stability analysis of flows in a higher Reynolds number regime, in order to estimate the

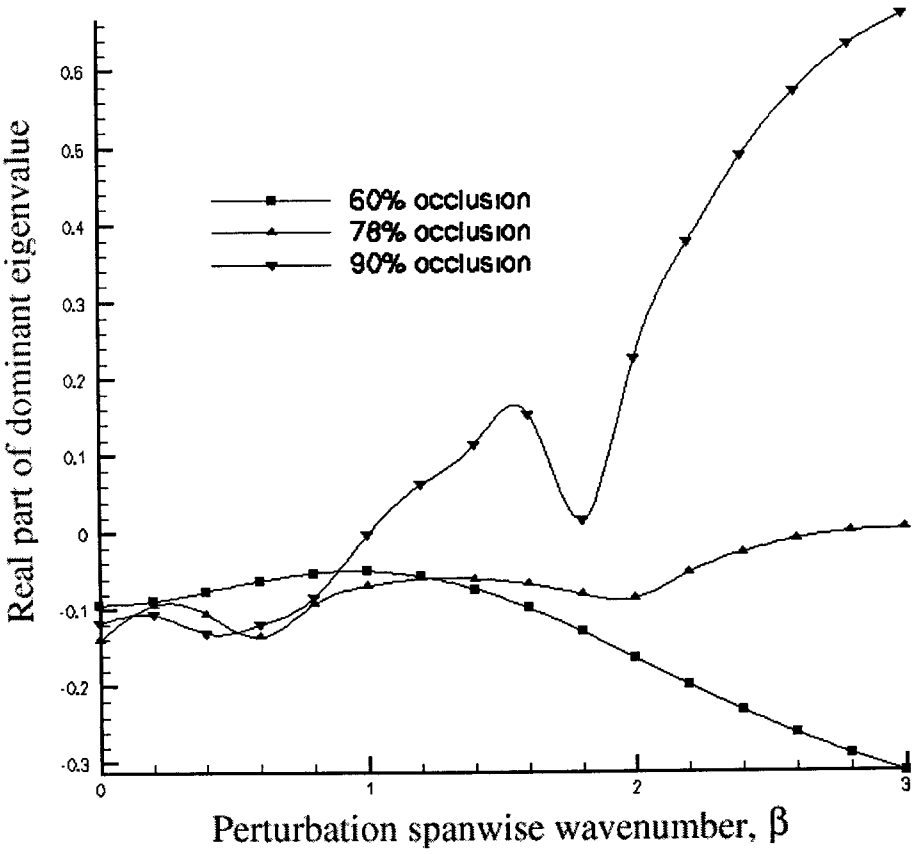

Figure 5: Plot of real part of dominant eigenvalue against spanwise wavenumber β for 60%, 78% and 90% stenoses at a fixed Reynolds number of 150

onset of three dimensionality. We hope to also get a feel for the nature of the instability and for the flow immediately after its development.

Figure 3 shows the value of the real part of the dominant eigenvalue as a function of the stability parameters Re and the spanwise wavenumber β, for the 60% occluded stenosis model. It is immediately seen that the effect of increasing the Reynolds number is a destabilising one, as the curve is essentially shifted upward in the direction of larger real part. The peak, at a wavenumber of around 1.6 corresponding to a spanwise disturbance wavelength of $3.9D$, seems very much geometry dependent, and appears invariant of Reynolds number. The onset of three-dimensional instability arises at a Reynolds number falling between 250 and 300, nearer to the 300 side. Figure 4 depicts the out-of-plane perturbation velocity field of the dominant eigenmode of the nearest calculation to this instability. It is clearly a three-dimensional mode, and its growth corresponds to the loss of translation symmetry in the z-direction. The pairing of areas of velocity into and out of the page would imply some rotation about an axis aligned parallel to the x-direction. Further insight will be provided by plotting the full three-dimensional perturbation field, and by performing a three-dimensional Navier-Stokes simulation of the flow just beyond the instability. Figure 3 also appears to show two additional longer wavelength instability modes arising as the Reynolds number is increased. These lie at spanwise wavenumbers of approximately 0.2 and 0.6, and will become unstable at slightly larger Reynolds numbers than those included in the figure. It would be interesting to ascertain whether or not these would have an effect (through non-linear interactions) on the primary instability.

The majority of the eigenvalues obtained are real, but some of those corresponding to $0.4 \leq \beta \leq 0.6$ are complex, contributing to the slightly erratic behaviour of the curves at these points.

Figure 5 shows the effect of stenosis extent on the real part of the dominant eigenvalues over the wavenumber range $0 \leq \beta \leq 3$. The dominant eigenvalue is plotted for each of the 60%, 78% and 90% occluded channels with a steady base flow at a Reynolds number of 150. Continuing the trend shown in Figure 3 the 60% occluded base flow is stable to three-dimensional perturbations at $Re = 150$. However, the effect of increased stenosis is to destabilise the flow. It can be seen that the peak real eigenvalue becomes greater with each constriction of the channel. With 90% occlusion the dominant eigenvalue clearly crosses the positive real axis and the flow becomes unstable to three-dimensional perturbations. Additionally, the shortening of the stenosis length scale causes the disturbance wavelength of maximum instability to similarly shorten, marked by the movement of the real eigenvalue peak to the right. Further calculation to extend the β range of this graph and locate the peak is warranted. An interesting point to note is that whilst the 60% case yields real eigenvalues at its three-dimensional instability, the 90% case displays complex eigenvalues.

The two-dimensional base flows used in these calculations are presented in Figure 6. The flow through the 60% stenosis is just mildly asymmetric, whereas the (still stable) 78% occlusion shows much more deviation from plane Poiseuille

flow. It is perhaps inevitable that the 90% occluded base flow is unstable, as it contains a standing vortex that would have a tendendy to amplify disturbances by inducing further movement of itself via the velocities induced by its image vorticity.

Floquet analysis of time-periodic base flow

Preliminary results have been obtained concerning the stability of a two-dimensional flow driven by an oscillatory volumetric inflow rate. The parallel inflow, an approximation to plane Womersley flow, is given by

$$u(y,t) = \frac{3}{2}\left(1 - \frac{y^2}{R^2}\right)\left(1 + \frac{3}{4}\sin(\omega t)\right) \qquad (10)$$

where R is the channel half-height and ω the angular frequency. The inflow at any time is thus instantaneously equivalent to plane Poiseuille flow with a Reynolds number of $[1 + 3/4\sin(\omega t)]/\nu$. ω is chosen to provide a desired Womersley number, α, according to the relationship:

$$\alpha^2 = \frac{R^2\omega}{\nu} \qquad (11)$$

Figure 7 shows the two-dimensional flow within the 60% occluded geometry at the peak inflow (at a quarter of a cycle) of a calculation with $\alpha = 4$ and Re, based on temporally and spatially averaged inflow velocity, equal to 150. The flow is symmetric and remains so throughout the entire cycle. However, in direct analogy to the steady case, we would expect increasing the Reynolds number to at some point result in a bifurcation in which this symmetry is broken.

A full-period Floquet stability analysis finds that, as we would expect for a converged flow, the dominant multiplier associated with a $\beta = 0$ (two-dimensional) perturbation has magnitude less than unity. An unstable two-dimensional mode would be permitted to grow in the two dimensional Navier-Stokes simulation through which the base flow is determined. Quantitatively, for these conditions the dominant multiplier is real, of magnitude 0.79. This is of interest as we previously showed in Figure 6 that the steady flow of $Re = 150$ through this geometry was mildly asymmetric. Thus, as far as the initial asymmetry bifurcation is concerned and comparison can be drawn, the effect of pulsatility of the inflow is stabilising.

Contours of the vertical (x-axis symmetry breaking) velocity field associated with the dominant, stable eigenmode at the beginning of the cycle are depicted in Figure 8, together with selected two-dimensional streamlines. This is an asymmetric mode and is believed to be the mode of the symmetry breaking bifurcation for the periodic flow case. Figure 9 shows the vertical velocity distribution of the base flow at a Reynolds number of 200, at 11/16 of the cycle, where the asymmetry is clearly visible.

It's onset will be accurately determined by using symmetry boundary conditions along the channel centreline to constrain the flow and subsequent Floquet stability analysis. This BiGlobal stability analysis will also be used to calculate the onset of three-dimensionality within these periodic stenotic flows, and the effects of inflow frequency on these instabilities.

CONCLUSIONS

The method of BiGlobal stability analysis has successfully been applied to the study of stenotic channel flows of interest from the perspective of biomedical research. It has been shown that there are instabilities arising within these stenotic geometries within a Reynolds number range that can be well resolved by our spectral/*hp* element method, and that our method yields eigenvalues and instability modes of high accuracy. The instability leading to three dimensionality in a 60% occluded channel has been isolated, and the effect of increasing the extent of the stenosis has been demonstrated. The existence of further instability modes at higher Reynolds numbers has also been shown. In addition, the method has been applied to the study of initial bifurcation to asymmetry of a periodic flow solution. These ground-breaking calculations have demonstrated the applicability of the method to locating the onset of asymmetry in the periodic flow through a stenotic channel, and pave the way for finding the onset of three-dimensionality, and for calculations in the near future assessing the stability of axisymmetric stenotic flows.

ACKNOWLEDGEMENTS

The authors would like to thank Dwight Barkley of the University of Warwick for furnishing us with his FloK code upon which ours is largely based, and EPSRC for funding Robin Pitt's studies.

REFERENCES

Caro, G. C., Fitz-Gerald, J. M., and Schroter, R. C., 1971, "Atheroma and Arterial Wall Shear - Observation, Correlation and Proposal of a Shear Dependent Mass Transfer Mechanism for Atherogenesis" *Proceedings of the Royal Society of London, Series B*, Vol. 177, pp. 109-159.

Nerem, R. M., Cornhill, J. F., 1980, "The Role of Fluid Mechanics in Atherogenesis", *ASME Journal of Biomechanical Engineering*, Vol. 102, pp. 181-189.

Schatz, M. F., Barkley, D., and Swinney, H. L., 1984, "Instability in a Spatially Periodic Open Flow", *Physics of Fluids*, Vol. 7, pp. 344-358.

Sobey, I. J., and Drazin, P. G., 1986, "Bifurcations of Two-Dimensional Channel Flows", *Journal of Fluid Mechanics*, Vol. 171, pp. 263-287.

Theofilis, V., Barkley, D., and Sherwin, S. J., 2002, "Spectral/*hp* Element Technology for Flow Instability and Control", *Aeronautical Journal*, Vol. 106, pp. 619-625.

Theofilis, V., 2003, "Advances in Global Linear Instability of Nonparallel and Three-Dimensional Flows", *Progress in Aerospace Sciences* (to appear).

Tuckerman, L. S., Barkley, D., 2000, "Bifurcation Analysis for Time-Steppers", *Numerical Methods for Bifurcation Problems and Large-Scale Dynamical Systems*, Doedel, E. and Tuckerman, L. S., ed., Springer, New York, pp. 543-566.

(a)

(b)

(c)

Figure 6: Vorticity field of steady two-dimensional base flow at $Re = 150$ for cases with (a) 60%, (b) 78% and (c) 90% stenosis

Figure 7: Vorticity distribution at 1/4 cycle for periodic flow with $\alpha = 4$ and $Re = 150$

Figure 8: Countours of vertical velocity and streamlines of dominant two-dimensional Floquet mode for periodic flow with $\alpha = 4$ and $Re = 150$

Figure 9: Vertical velocity distribution at 11/16 cycle for periodic flow with $\alpha = 4$ and $Re = 150$